Characterizing the Molecular Structure of Preceramic Polysiloxanes for Freeze Casting of Silicon Oxycarbide Ceramics

Thesis by

Ankita Nandi

In Partial Fulfillment of the Requirements for the degree of

Bachelor of Science in Materials Science

CALIFORNIA INSTITUTE OF TECHNOLOGY

Pasadena, California

2024

© 2024

Ankita Nandi

All Rights Reserved

ACKNOWLEDGEMENTS

First, I would like to thank my graduate student mentor, Dr. Laura Quinn. Thank you for guiding me through every step of the process ever since I joined the group, and being my biggest supporter throughout this entire thesis. I have seen how much I have grown as a scientist, communicator, and researcher, much of which has been due to your mentorship and leadership.

I am also extremely grateful to my advisors, Professor Katherine Faber and Professor George Rossman. Thank you for both for answering my endless questions and helping me grow as a researcher. Professor Rossman, thank you for welcoming me as a research student and helping me explore the opportunities for interdisciplinary research that has continued into this thesis process. Professor Faber, thank you for being my advisor since I stepped foot on Caltech campus, and welcoming me into the group. Being a part of the Faber Group has been an remarkable experience that has made my undergraduate years truly invaluable, and I really appreciate how much you have helped me grow in these past four years.

To all members of the Faber Group, thank you for discussion, encouragement, and welcoming me as a part of the group – Kevin, Zac, Sara, Wes and Seneca. I learn something new everyday from each of you, and I am so grateful for the opportunity to know each of you individually. Seneca, thank you for helping me with the DSC measurements, and thank you everyone for helping me puzzle through confusing results whether in group meetings or in the office.

Thank you to Dr. Chi Ma for providing guidance in the SEM, and to Dr. David Vander Velde for your expertise in NMR and answering all of my questions. Additional thanks to Professor Julie Kornfield for your polymer expertise and helping me understand what I should be looking

for. Thank you to Dr. Erin Burkett for helping me communicate and fine tune my language in the writing and editing of this thesis.

Lastly, I have endless gratitude for my friends and family who have been my biggest supporters through the research, analysis, and writing of this thesis, and throughout my four years at Caltech. Your belief has been insurmountable and I cannot thank you enough for that.

ABSTRACT

Preceramic polymers are frequently used as a lower energy intensive precursor for creating ceramics, as they can be transformed into robust ceramics at lower temperatures than is required by traditional processing routes. Additionally, preceramic polymers can be used to produce structures with microstructural variability, such as porosity. Polysiloxanes are one type of preceramic polymer that have been used to create silicon oxycarbide materials. Previous research has utilized polysiloxanes in freeze casting to create porous ceramics, specifically investigating development of different pore morphologies and pyrolysis profiles. However, there has been little exploration into the differing molecular structures of various polysiloxanes impact their behavior through the freeze casting process. Investigating the molecular structure of commonly used proprietary polysiloxane Wacker SILRES® MK has provided some insight into molecular structural changes during the freeze-casting process. These can be used to improve freeze-casting microstructure from another proprietary polysiloxane, Wacker SILRES® H44. MK and H44 were characterized in powder, solution, and post pyrolysis stages of the freeze casting process. Techniques including FTIR-ATR spectroscopy, Raman spectroscopy, NMR spectroscopy, DSC, and SEM imaging were used to determine how to improve the robustness of freeze cast structures made with H44. MK was determined to be a polymethylethoxysiloxane, and H44 to be a polymethylphenylsiloxane. The high energy and high steric strain phenyl groups in H44 require additional energy to facilitate crosslinking during the freezing process for H44. Both MK and H44 converted to silicon oxycarbide upon pyrolysis. Adding crosslinker improved the desired porous microstructure and robustnesss of freeze-cast structures made with H44, as evidenced by SEM imaging. Future exploration into other preceramic polymers should consider the impact of high energy functional groups upon the processing methods to create desired microstructures.

TABLE OF CONTENTS

TABLE OF FIGURES

Introduction

Ceramics are high-temperature resistive, high-strength and environmentally stable materials, used in aerospace applications, water treatments, electronic and battery materials, and biomaterials such as tissue scaffolds and false teeth[1–8]. However, traditional methods of creating ceramic structures are energy intensive. Robust ceramics must be sintered at temperatures between 1700°C-2000°C and may require the incorporation of fillers for functional properties[5,9]. Preceramic polymers are of interest because they use polymers to create ceramic structures, which are referred to as polymer-derived ceramics. Using polymers diversifies the ceramic creation process, because well-known manufacturability and handling techniques developed for polymers can be applied to preceramic polymers, and many only require 1100°C-1300°C compared to the high temperature required for non-polymer-derived ceramics[5,9]. These polymer-derived ceramics have been used as fibers for composite materials, matrices for composite materials, coatings, and more[9].

Preceramic polymers can be processed through polymer processing techniques, such as extrusion or molding[9]. Following shaping, the preceramic polymer structures are fired through a sintering or pyrolysis step, or firing the structures in an inert environment at a high temperatures to transform the polymer into a ceramic. The pyrolysis decomposes the polymer and converts the material into a ceramic, increasing the mechanical strength and ensuring that the structure remains chemically inert[9,10]. Specifically, the pyrolysis decomposes the polymer to remove hydrogen and methane molecules, leaving behind a carbide structure[11]. Given the lower working temperature range of polymers, much lower than of traditional ceramics, which ranges from 1700°C-2000°C, preceramic polymers can be used to create strong, thermally stable structures without the high

energy input required in traditional ceramics processing. With preceramic polymers, ceramics can be created in a much less energy-intensive way than other ceramic processing techniques require[9].

Polysiloxanes are a type of preceramic polymer commonly used due to their commercial availability, high ceramic yield and carbon content, and ease of processing[12]. Polysiloxanes have a low glass transition temperature, low surface tension, and can still remain liquid even with high molecular weights[13]. Figure 1 shows a generic polysiloxane structure, highlighting the characteristic Si-O backbone. A well-known polysiloxane is polydimethylsiloxane, or PDMS. PDMS is well-known for its biocompatibility, optical transparency, chemical stability and gas permeability, making it a well-suited material for microfluidics and biological applications[14]. As a preceramic polymer, polysiloxanes have been used to create silicon carbide or silicon oxycarbide structures[12,15]. Specifically, polysiloxane has a high ceramic yield and strong crosslinking thermosetting[16] that makes it an ideal precursor, given the silicon backbone and flexibility of the Si-O chain allowing for easier crosslinking. This dense crosslinked structure prevents rearrangement during sintering, and the Si-O bond in a polysiloxane is high energy, therefore preventing decomposition of the backbone.

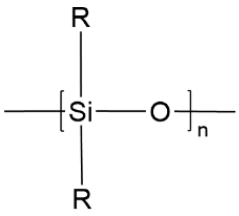

Figure 1. Polysiloxane structure. R indicates different functional groups off the Si on the Si-O backbone.

Preceramic polymers can produce structures with microstructural complexity by introducing features such as porosity, which can allow for other functional properties such as heat

transfer, mimicking cellular environments, and increased permeability[12,17]. Porous ceramic applications include battery separators, artificial bones, and gas permeable materials[4,5,18]. Porous structures are advantageous for such applications because of flow capabilities of other materials through the structures, and ceramics are preferable due to their high thermal stability and chemical inertness. Porous ceramics are therefore ideal for variable flow and high strength applications.

There are multiple ways to manufacture porous polymer-derived ceramics. These methods include replica templates, direct foaming, and sacrificial template. In replica methods, a physical "template" is inserted into a ceramic suspension or solution and removed through firing a dry, templated solution. Direct foaming introduces air or another gaseous species into the suspension or solution to create a porous structure. The sacrificial template disperses a sacrificial material into a ceramic solution or suspension which is removed via heat or sublimation. [19]

One method of using the sacrificial template method is freeze casting. Figure 2 depicts the freeze casting process, going from a polymer solution, to a freeze-dried polymer structure, to the final ceramic structure.

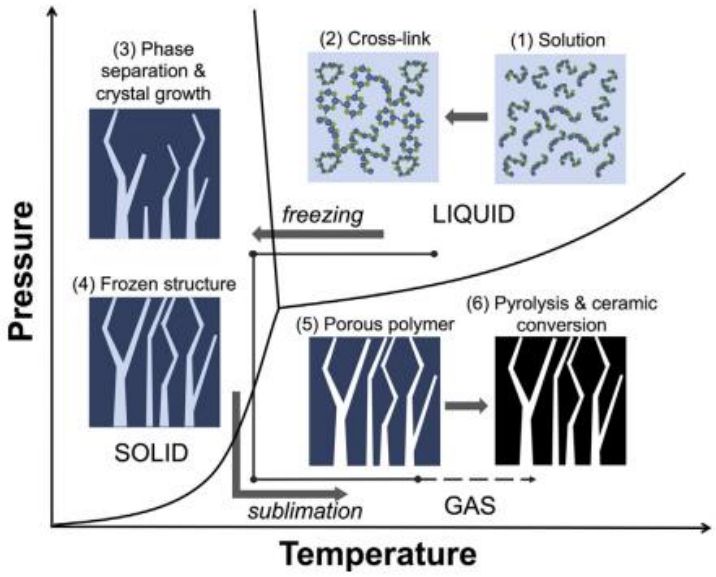

Figure 2. Schematic of solution-based freeze-casting process, illustrating the changes in phases step to step. Phases describe phase of solvent. In pyrolysis, porous polymer transforms into inorganic material. From [3].

When dissolving the polymer, either liquid or powder, in the solvent, a crosslinker is added during dissolution so that the polymer crosslinks and forms interconnecting bonds, leading to a strong final structure. The freezing results in a solid structure of polymer in a porous framework. Specifically, the solution is directionally frozen, resulting in a phase separation between the polymer and solvent as solvent crystals form. The shape of the crystals, resulting from the frozen solvent, controls the pore shape and depends on the interactions between the solvent and solute. After freezing, the solvent crystals are then sublimated away from the structure in a freeze dryer, resulting in a polymeric porous solid. The solid is pyrolyzed to induce the transition from the polymer material into the final ceramic[12]. During the final pyrolysis part of freeze casting, polysiloxanes are transformed into silicon oxycarbide.

Directional pores can be created by controlling the freezing front velocity and the temperature gradient during freezing, and the solvent used in the freezing solution creates

structures with distinct pore morphologies[12,19,20]. The ability to customize pore morphologies therefore lends freeze casting an advantage over techniques like direct foaming, which only produces spherical pores[19]. Additionally, higher mechanical strength has been observed in freeze cast structures compared to ceramics produced with the replica method, which may have cracks in the porous structure, as the method relies on a solution or suspension filling a mold, which could result in weak areas or not fully filled areas[15].

The effects of freezing conditions and solvents used in freeze casting on pore morphologies have been well-explored, but less research has been done on the changes to preceramic powders at different stages of the freeze-casting process[8,12,19–21]. Thus, this thesis serves to understand changes in molecular structural properties for two preceramic polymer powders, specifically polysiloxanes, for successful freeze casting, starting with powder analysis and continuing to analyze powder behavior in solution, after freezing, and after pyrolysis.

Although multiple polysiloxanes are available commercially, a commonly used preceramic polysiloxane is Wacker SILRES® MK[12,19–21]. Another polysiloxane powder, Wacker SILRES® H44, is also available and has a higher carbon content, but is not typically used due to poor performance in freeze casting. It is less clear why freeze casting Wacker MK creates a robust silicon oxycarbide structure, but using H44 does not result in a similarly robust structure with well-defined pores.

One possible reason for differences in successful freeze casting of the proprietary polymers could be due to differences in the molecular structure. Characterizing the polysiloxanes to determine the molecular structure helps determine whether these are a driving factor in successful freeze casting, and whether certain functional groups might be preferable for freeze casting.

Additionally, each proprietary polymer has a “best by” date and the polymers have shelf lives of about one year, but the reason for this shelf life is not published[22]. The main difference between Wacker MK and Wacker H44 are that MK is a methyl-functionalized polysiloxane[22], while H44 is a phenyl-functionalized polysiloxane [23]. As proprietary polymers, not much information is available about the specific structures or functionalization of the molecules. Figure 3 shows possible structures of Wacker MK and Wacker H44 based off the limited molecular structural information given by Wacker.

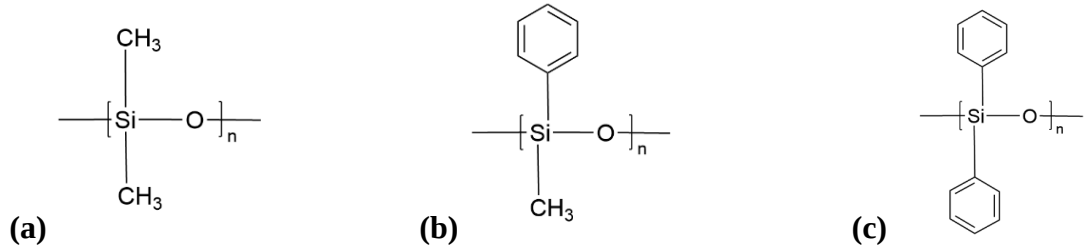

Figure 3. (a) polydimethylsiloxane: both functional groups off the Si-O backbone are methyl groups; **(b**) polymethylphenylsiloxane: the Si-O backbone has one methyl functional group and one phenyl functional group; **(c)** polydiphenylsiloxane: the Si-O backbone has two phenyl groups

The Wacker MK and Wacker H44 polymers were analyzed using FTIR-ATR (Fourier Transform Infrared – Attenuated Total Reflectance) and Raman spectroscopy throughout the freeze-casting process to understand the chemical bond and structural changes the polymers undergo during freeze casting to become the final silicon oxycarbide structures. Both techniques are non-destructive and can be used to identify different functional groups present in the polymer molecules. Through identifying the different functional groups present, we can better understand why Wacker MK successfully creates freeze-cast structures, and how we can improve the pore characteristics of structures made with H44.

FTIR-ATR was used to observe the difference in reflectance of light upon hitting the sample. The high frequency region of FTIR spectra can be used to identify main functional groups, while the low frequency region helps identify aromatic groups and can be used as a "fingerprint" region as there are distinctive peaks of the different bonds of different molecules in this region in comparison to the high frequency region. FTIR is a common technique for analysis of polymer structural bonds and properties, as it is sensitive to different bending and stretching behaviors of the structural bonds, which are unique to each bond and molecule and can therefore be used to identify bonds in that way[12,24–27]. Specifically, structural bonds and functional groups are excited at different infrared wavelengths, and results in differences in reflectance from these excitations. From Raman spectroscopy, vibrational modes of the polymer indicated by the Raman shifts are excited by different symmetrical bonds in the molecule. These Raman shifts are also characteristic of different bonds in the structures. Furthermore, the "free" carbon evolution of the polymer between the powder and the final freeze-cast structures was evaluated[9]. This "free" carbon evolution demonstrates the final ceramic yield and can confirm whether the final freeze cast structure has converted to some form of silicon carbide or silicon oxycarbide. Similar to FTIR, Raman spectroscopy is also a common way to identify different bond vibrations and can be used to identify bonds present in the polymer structures[27,28]. Thus, Raman spectroscopy and FTIR-ATR were used in conjunction with each other to identify the different functional groups in each polymer powder.

Although limited information is available regarding the Wacker MK and H44 polymer compositions, spectra for poly(dimethylsiloxane) (PDMS) and poly(diphenylsiloxane) (PDPS), structures shown in Figure 3a and 3c, respectively, were consulted as references for the MK and H44 powders, as these are polysiloxanes with exclusively methyl and phenyl functional groups,

respectively. Identifying the common peaks between these reference materials and the analyzed powders will allow us to determine the main functional groups and differences that may impact the polymer behavior during freeze casting. Given the limited knowledge available about the proprietary polymers, Figure 3b shows polymethylphenylsiloxane, which may serve as an intermediary structure between PDMS and PDPS as the likelihood of two phenyl functional groups is low due to the high energy required for the molecule creation, given the strain effects of the phenyl group in comparison to methyl groups[29].

Solution state nuclear magnetic resonance (NMR) and differential scanning calorimetry (DSC) were also used to determine molecular structure of the polymers and its impacts on processing. NMR allows us to observe the carbon and oxygen bonds present in the molecule, further determining the structure, and interactions with the solvent in the freeze-casting process. For the purposes of this thesis, we characterized the polymers when dissolved in cyclohexane, as it is a common solvent used in freeze casting. DSC gives information about heat flow at different temperatures and can be used to determine phase transitions, such as glass transition and melting temperatures. Additionally, these properties will give information about the monomer count and polymer chain length in the polysiloxanes. These characteristic properties can be used to identify functional groups present in the proprietary polymers, and how they may impact behavior of the preceramic polymers during the freezing process. Through the powder and solution analysis, we can further understand preceramic polymer behavior and interactions throughout the freeze-casting process that impact the creation of successful freeze-cast structures. We also observed how the crosslinker impacts polymer behavior once in solution, as a crosslinked solution is placed in the freeze casting mold before being frozen. These solutions will also be characterized with the FTIR-

ATR and Raman to determine whether any changes occur in the polysiloxane structure as observed with those methods, separate from the peaks of the cyclohexane and crosslinker.

To complete our analysis of the polysiloxanes through the freeze-casting process, the final freeze-cast structures with the FTIR-ATR and Raman were characterized. Specifically in the case of H44, given the lack of previous work using H44 in freeze casting, this final stage of analysis will allow us to determine what the final product was, and compare that to the final composition of freeze cast structures made with MK[12]. Through the characterization of preceramic polymer throughout the freeze casting process, this work seeks to improve our understanding of how the preceramic polymer molecular structure impacts the success of freeze casting as a pore forming process. With this better understanding of the impact of structure on freeze casting, potential solutions for improving the pore characteristics of H44 through freeze casting are presented.

Experimental Details

Materials Preparation

Spectra were collected on a Thermo-Nicolet iS50 FTIR, between 400 and 4000 cm^{-1}. Commercially available Wacker MK and Wacker H44 powder (Wacker Chemie) were analyzed as preceramic polymers, as solutions in cyclohexane, and as freeze-cast solids. As the Wacker materials are proprietary powders, little information about the polymer molecular structures or compositions was available. Powders were purchased in years ranging from 2016 to 2021.

Solutions composed of 20 wt% preceramic polymer powder and 80 wt% cyclohexane or cyclooctane were freeze cast by first dissolving the preceramic polymer in the solvent. Solutions

were each stirred for 10 minutes before adding 1 wt% of Wacker GF91 crosslinker (Wacker Chemie) and stirring for another 5 minutes to facilitate crosslinking. The crosslinking solution was degassed for 10 minutes to prevent air bubbles during freezing, then froze until the temperature reached -30 ℃. The frozen structures were placed into a freeze dryer (VirTis AdVantage 2.0, SP Scientific, Warminster, PA, USA) to sublimate the solvent and leave behind the templated polymer. After freeze drying, the polymers were pyrolyzed at 1100 ℃ in argon for 4 hours heating and cooling using a ramp rate of 4C/min to transform into ceramic[12]. H44 solutions with 2 wt% crosslinker in cyclooctane were also freeze cast using the same process.

PDMS was used as a reference to compare the powders in the FTIR-ATR and Raman spectroscopy methods. PDMS has a known polymer structure that can distinguish similar peaks and identify patterns across the different spectra and polymers to help identify key structural features in MK and H44.

Characterization

Fourier transform infrared – attenuated total reflectance (FTIR-ATR) spectroscopy

FTIR-ATR is used to collect FTIR spectra from powders and liquids in intimate contact with a diamond surface. Unprocessed polymer powders were placed directly on the diamond surface when collecting spectra. The freeze-cast solids, both after freeze drying and pyrolysis, were ground into a solid powder using a diamond saw before collecting the spectra. Grinding the solid into powder with the saw ensured appropriate coverage of the collection area. Powders were pressed to the order of 10 kPa to ensure intimate contact with the diamond surface. Given that these samples were powder, a piece of aluminum foil was placed over the powder to ensure that no cross contamination of samples occurred between subsequent spectra collections. Solutions were placed directly on the diamond surface, with no foil, as they were already in intimate contact

with the diamond surface. A crosslinked PDMS sample was placed directly on the diamond surface and the spectrometer applied pressure before collecting the spectra.

Raman spectroscopy

Raman spectra were collected using a Renishaw inVia QONTOR micro-Raman Spectrometer System, with a 532 nm laser at full power under 50x magnification. Freeze-dried solid and pyrolyzed solids were ground into powders using a diamond saw before collecting Raman spectra. Grinding the solids into powders ensured sufficient signal was received from the material. Additionally, using powder prevented insufficient signal from the porous nature of the freeze-dried and pyrolyzed solid, where the laser may hit a pore rather than the material. Spectra of the polymer powders, freeze-dried solid powders, and pyrolyzed solid powders were gathered using an 1800 nm grating and collected between 0 and 1500 cm^{-1} or 0 and 4000 cm^{-1}. Spectra of the solutions and crosslinker were collected with a 785 nm laser at 10% power at 50x magnification, using a 3400 nm grating, and collected between 100 cm^{-1} and 3400 cm^{-1}. The 785 nm laser was used to prevent fluorescence when taking the spectra, and the restricted wavenumber range was due to equipment constraints. As Raman shifts are independent of excitation wavelength, powder spectra collected from the 532 nm laser were directly compared to the solution spectra.

Liquid NMR of preceramic polymer powders

^{1}H (proton) NMR spectra were collected on a Varian 600 MHz spectrometer. Wacker MK and H44 powders were dissolved in protonated cyclohexane, in weight concentrations of 38% and 12%. As cyclohexane only has a single residual ^{1}H peak at 1.38 and ^{13}C peak at 26.43 ppm, it was suppressed in the analysis. ^{13}C NMR was performed using a Varian spectrometer at 150 MHz for

MK and 100 MHz for H44 to determine chemical bonds to the carbon atoms in the polymer structures for both preceramic polymers. ^{29}Si NMR was performed using a Bruker spectrometer to confirm functional groups present in the Wacker MK preceramic polymer powder. All spectra were collected at 25°C with acquisition times ranging from 0.8 seconds to 2 seconds.

Differential scanning calorimetry (DSC)

DSC was performed on a Discovery 400 from TA Instruments. Polymers were pressed in a T-zero pan at 25 mL/min. The samples were analyzed in nitrogen gas and cycled three times between -40 ℃ to 200 ℃ at a constant heating and cooling rate of 5℃/min, and samples were equilibrated at each maximum and minimum temperature before the next temperature change.

Scanning Electron Microscopy (SEM) Imaging

SEM images were taken on a field emission scanning electron microscope (ZEISS 1550 VP). Samples were nonconductive and so were coated using a HR metal sputtering coater with 5 nm Pt prior to SEM examination.

Results and Discussion

Analysis of Polymer Powders

As Wacker MK and Wacker H44 are both polysiloxanes, Si-O bonds were expected to be present in both, and low wavenumber regions were examined to determine key functional groups present. Additionally, reflectance is dependent upon the vibrations of the polymer bonds as resulting from polarity. Thus, FTIR-ATR confirmed the presence of different polar or otherwise non-symmetrical bonds in the polymers.

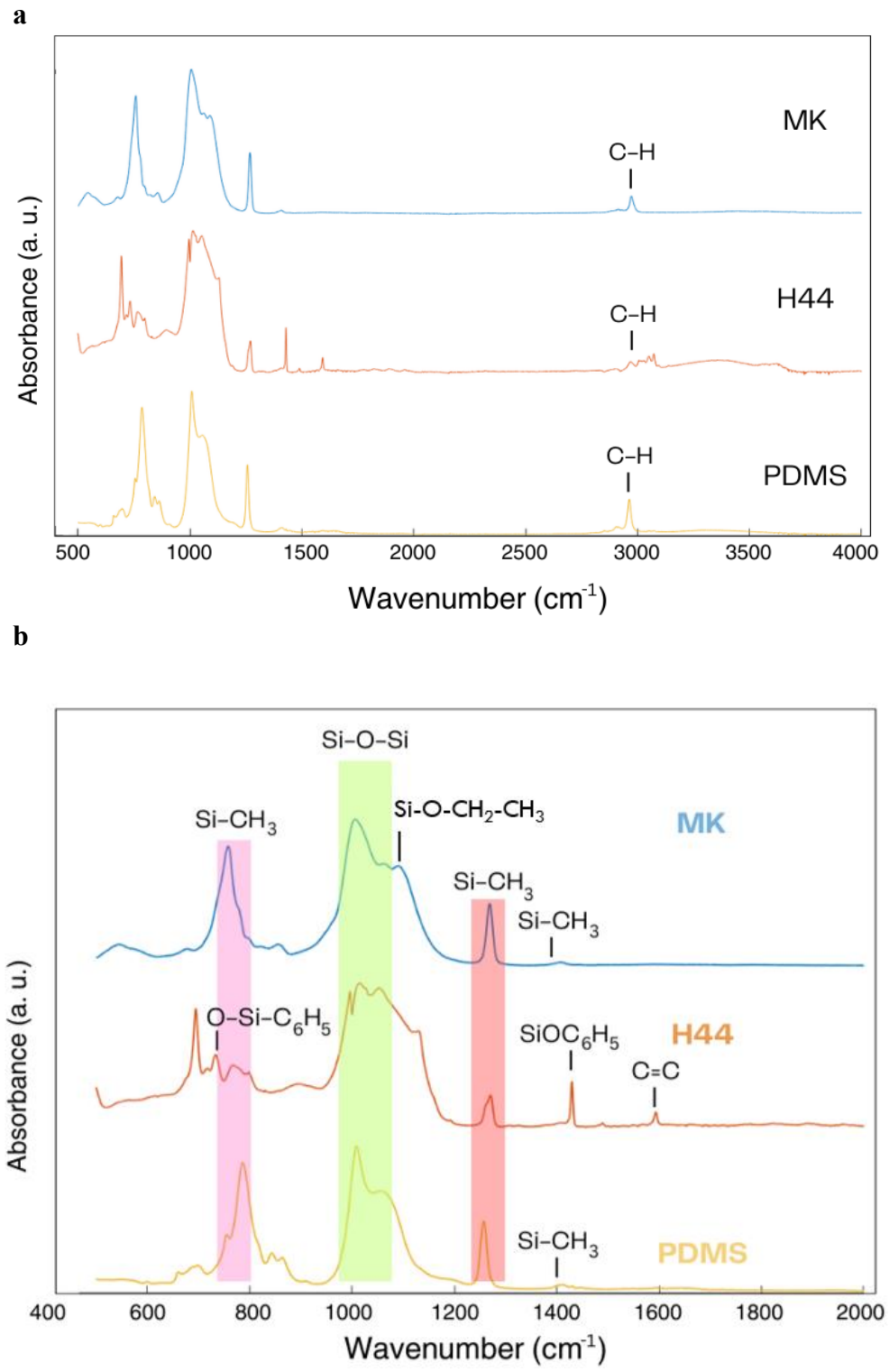

Figure 4. FTIR Spectra of MK, H44, and PDMS (a) spectra from 400 to 4000 cm^{-1}. **(b)** Enlarged spectra of (a) between 400 to 2000 cm^{-1} to highlight key identifying peaks.

PDMS is shown as a reference with well-known functional groups for comparison with the two proprietary preceramic polymers. As shown in Figure 4, both MK and H44 are clearly polysiloxanes, with strong peaks at 1000 cm^{-1}, indicative of the Si-O-Si stretch. MK, H44, and PDMS also all have a C-H stretch at 3000 cm^{-1}. Figure 4b enlarges the x-axis to focus on the "fingerprint" region and more clearly identify the different functional groups.

As seen in Figure 4b, the FTIR spectrum of MK has similarities to that of polydimethylsiloxane, or PDMS. This corresponds to the characteristic peaks found at 700, 1250 and 1450 cm^{-1} that indicate CH_3 stretches. Both MK and H44 also have Si-CH_3 stretches, indicating the presence of methyl functional groups in both powders. In the MK spectra, there is a shoulder on the peak at 1200 cm^{-1} that indicates the presence of either a second Si-O-Si stretch or a C-O-C stretch. Specifically, the shoulder is indicative of an ethoxy group off the Si-O backbones, as there is an additional peak that corresponds to the C-O-C stretch present in an ethoxy group. In the H44 spectra, there are peaks at 1450 cm^{-1} and 750 cm^{-1} that are indicative of a phenyl group off the Si-O backbone, which are absent in the MK spectra, confirming phenyl functionalization in H44 and the lack of phenyl groups in MK and PDMS.

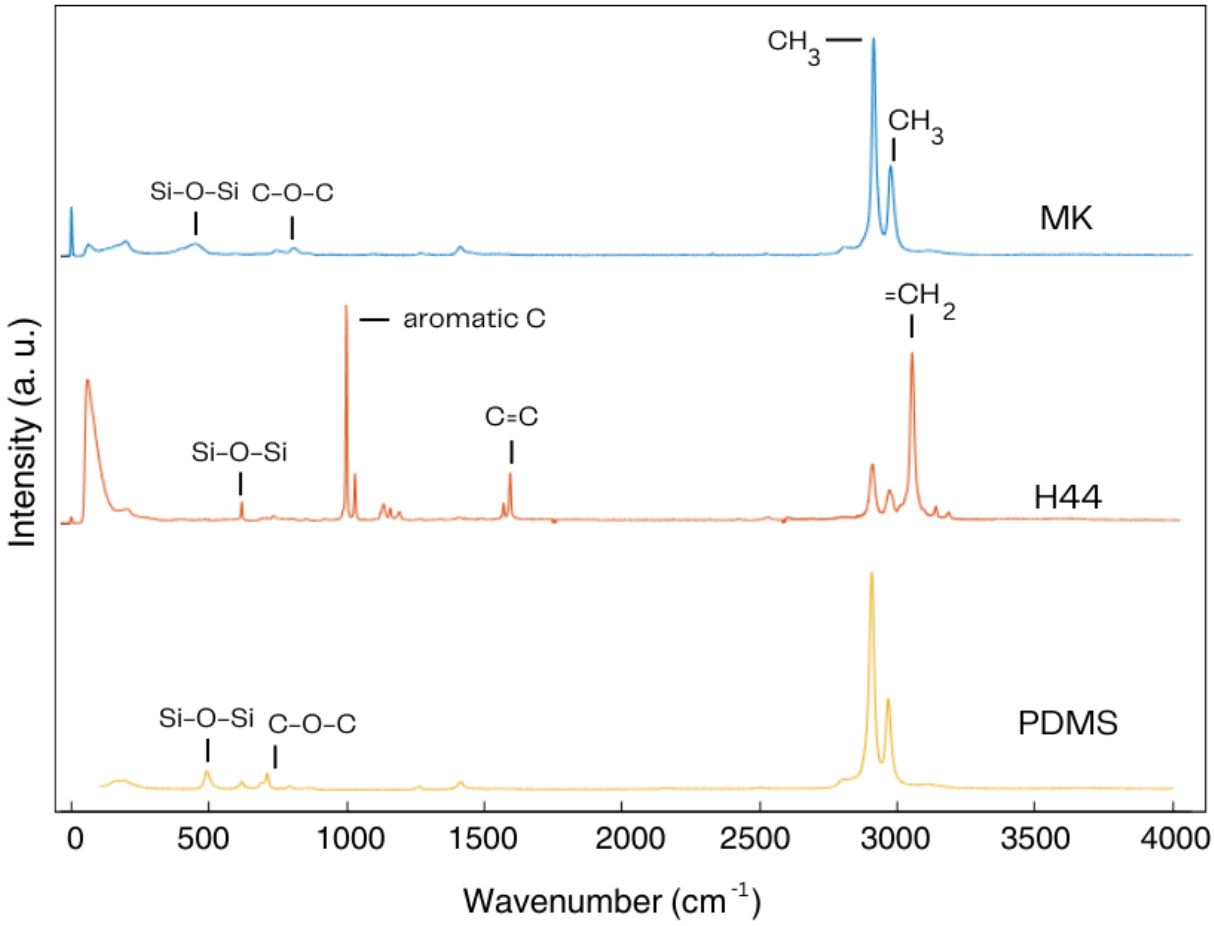

Figure 5. Raman spectra of MK, H44, and PDMS. Key bonds are labelled.

The Raman spectra confirmed different symmetrical bonds. All the polymers shown in Figure 5 had symmetrical CH_3 and Si-O-Si stretches. However, those are the only key peaks in the MK and PDMS spectra, which were similar to the IR spectra (Figure 4) as well, in comparison to other prominent peaks in the H44 spectra. Figure 5 distinguishes the symmetrical bonds that exist in the H44 polymer compared to the MK and PDMS spectra. Specifically, as seen indicated in Figure 5, there were aromatic and double bonded carbons clear in the Raman spectra that were not strong in the IR spectra due to the symmetricity of the double-bonded carbon bonds. The FTIR more strongly excites more polar bonds, while the Raman will have stronger modes resulting from symmetric bonds. There was also evidence of a C-O bond in the MK polymer, but it was weakly

vibrating as the bond is polar and therefore not symmetrical and did not vibrate strongly in the Raman spectra.

The Raman and FTIR spectra therefore confirm MK to have a C-O, specifically in the form of an ethoxy group off the Si backbone, with the polymethylethoxysiloxane structure as shown in Figure 6.

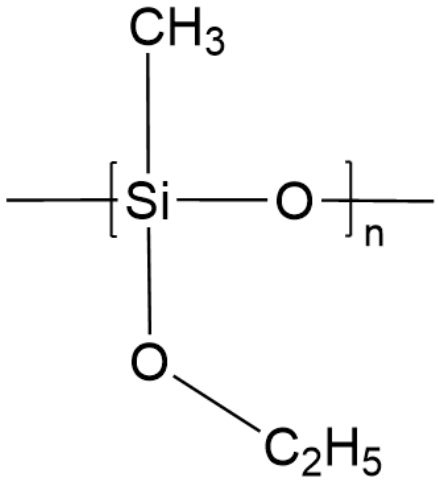

Figure 6. Polymethylethoxysiloxane molecule, with Si-O backbone, one methyl functional group, one ethoxy functional group, connected to the Si.

The Raman and FTIR spectra also confirm the H44 polymer to have both methyl and phenyl groups, therefore making it a polymethylphenylsiloxane.

Identification of functional groups from liquid NMR

Solution state NMR was also used to determine structural information about the polymers, as NMR determines chemical shifts that would indicate molecular structural characteristics. Given that polysiloxanes have mobile polymer chains due to the Si-O bond, and methyl groups were

likely to be present in both proprietary polymers, the proton spectra contributed structural information. ^{13}C and ^{1}H NMR was conducted on both H44 and MK. The ^{13}C and ^{29}Si reveal structural information about the polysiloxanes, specifically which functional groups and atoms are connected to carbons and off the silicon backbone. Figures 7a and 7b confirm the ethoxy group in MK as present in the proton and carbon NMR. The ^{29}Si NMR on MK confirms the ethoxy group directly attached to the Si atom. As shown in Figure 7a and 7b, the H44 NMR confirms the structure as deduced from the FTIR and Raman spectra. Deuterated cyclohexane has a single residual proton peak at 1.38 ppm. Although deuterated cyclohexane was not used in collecting the NMR spectra, the residual proton peak would be slightly larger than this peak. Similarly, the residual ^{13}C peak is slightly larger than 26.43 ppm, the residual peak for deuterated cyclohexane. These peaks are suppressed in the NMR analysis. The zero point of the NMR spectra is the peak shift of tetramethyl silane.

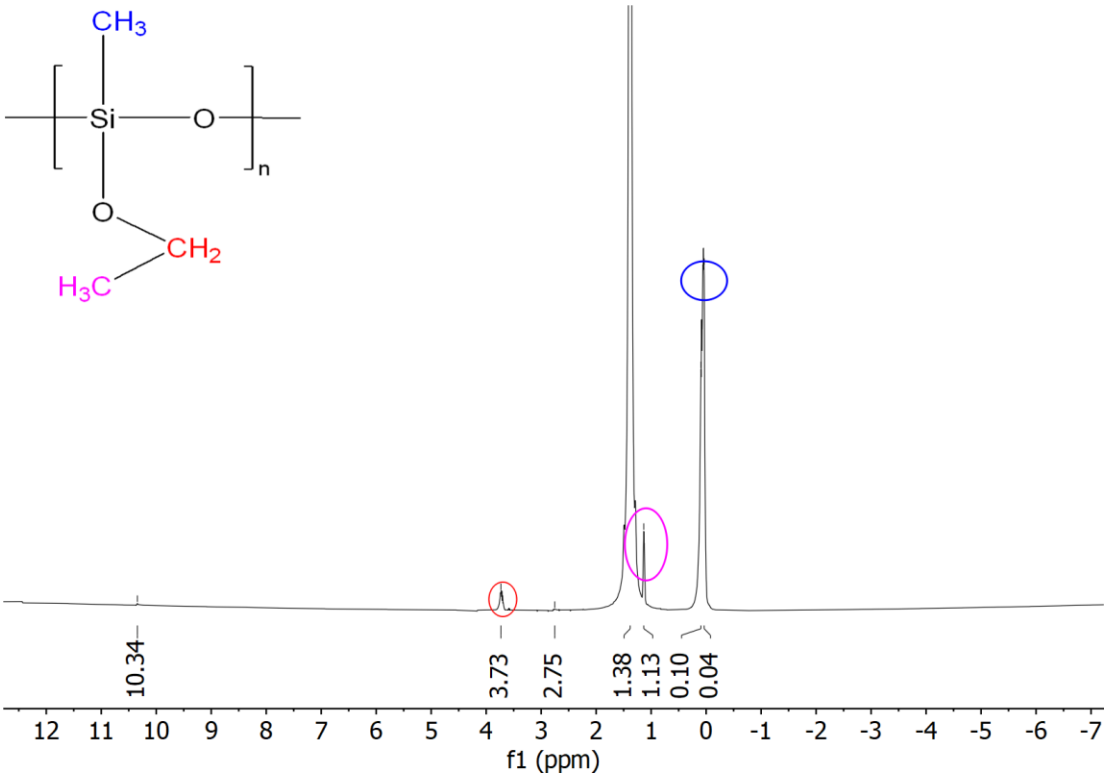
CH3
Si
O
n
O
CH2
H3C
10.34
3.73
2.75
1.38
1.13
0.10
0.04
12 11 10 9 8 7 6 5 4 3 2 1 0 -1 -2 -3 -4 -5 -6 -7
f1 (ppm)

(a)

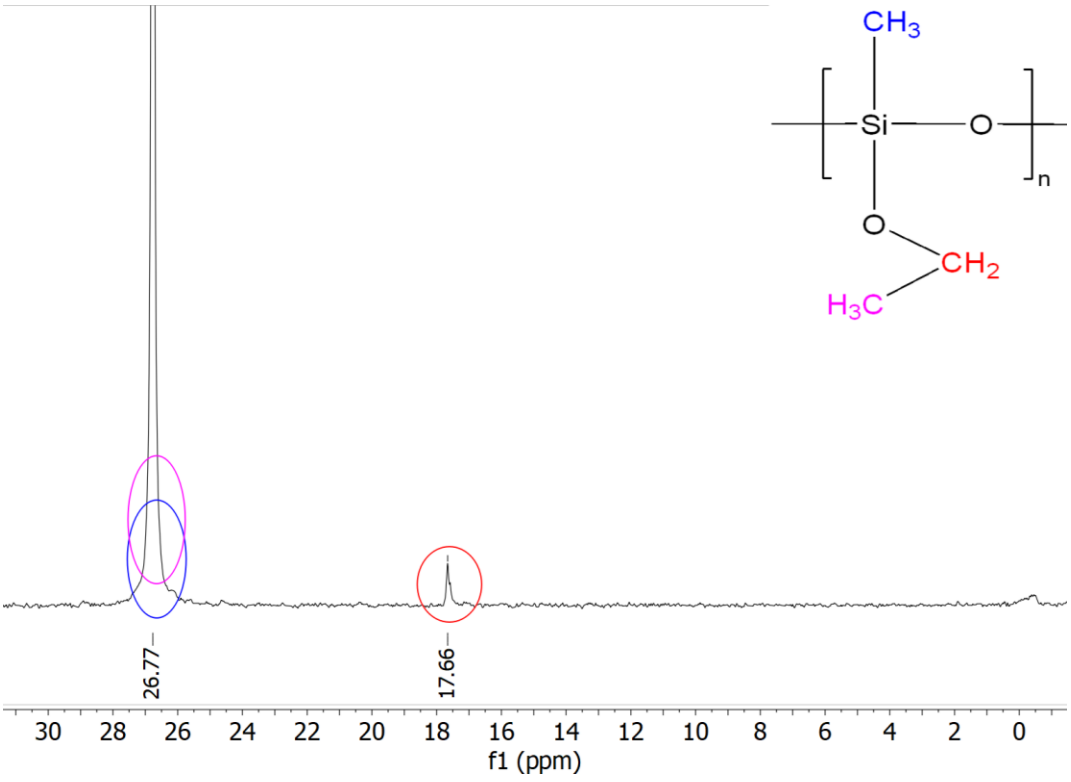
CH3
Si
O
n
O
CH2
H3C
26.77
17.66
30 28 26 24 22 20 18 16 14 12 10 8 6 4 2 0
f1 (ppm)

(b)

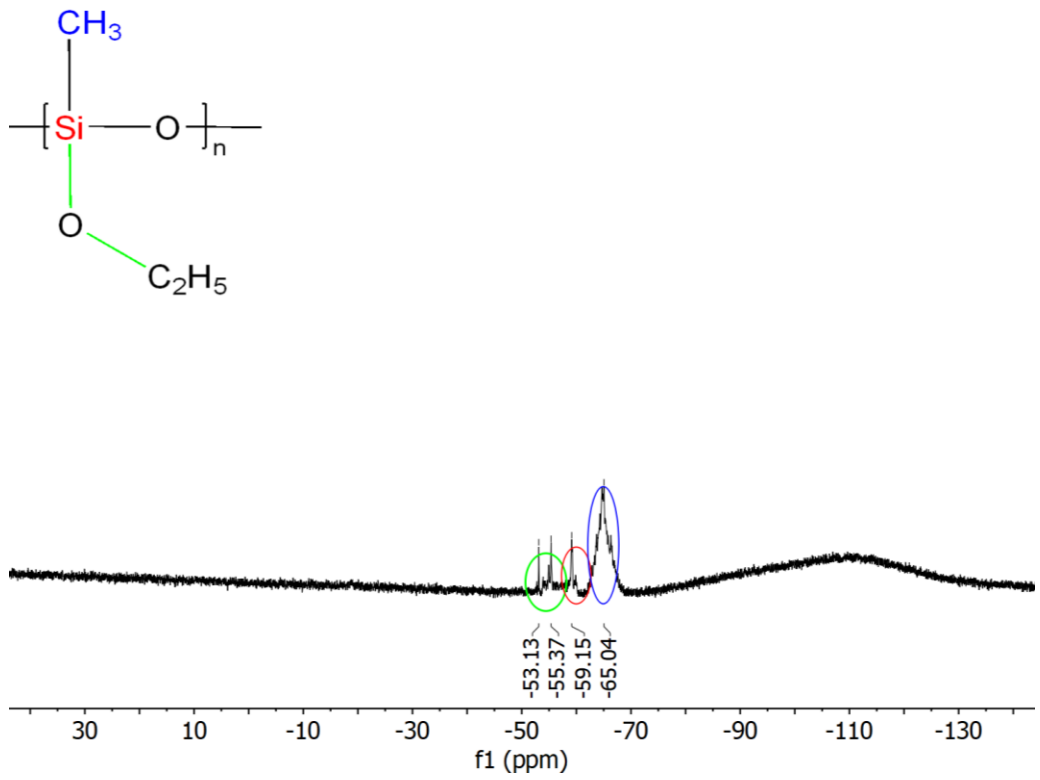
CH3
Si
O
n
O
C2H5
-53.13
-55.37
-59.15
-65.04
30
10
-10
-30
-50
-70
-90
-110
-130
f1 (ppm)

(c)

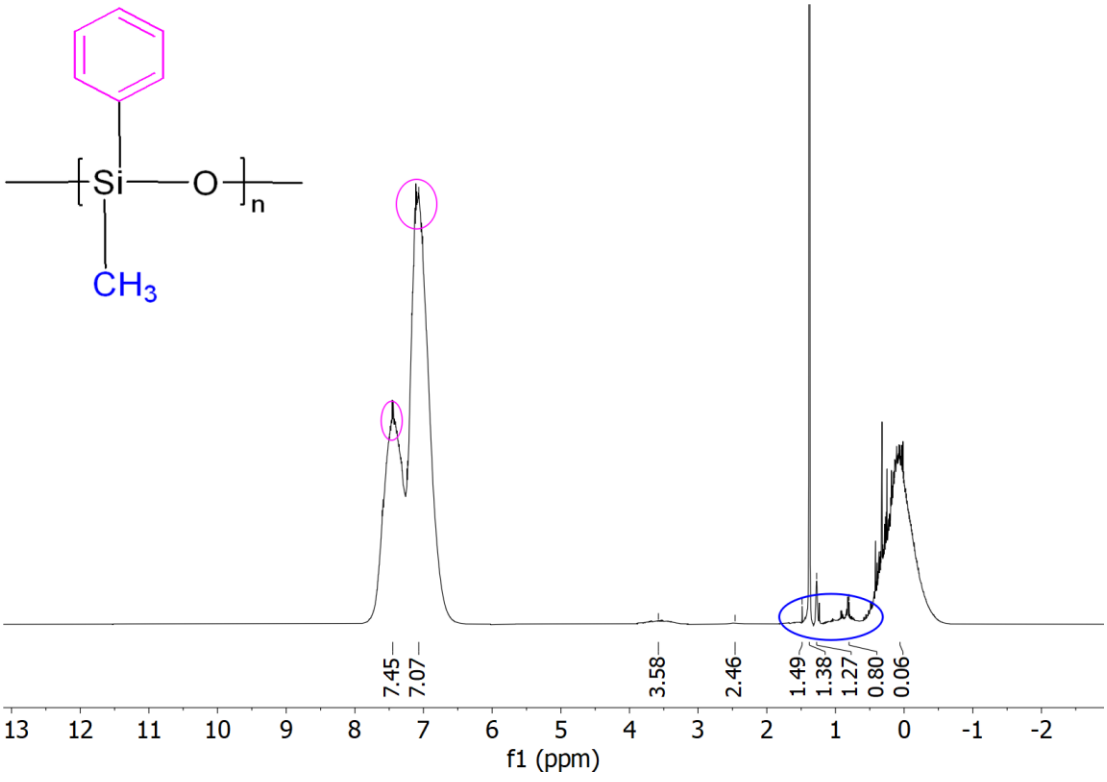
Si
O
n
CH3
7.45
7.07
3.58
2.46
1.49
1.38
1.27
0.80
0.06
13
12
11
10
9
8
7
6
5
4
3
2
1
0
-1
-2
f1 (ppm)

(d)

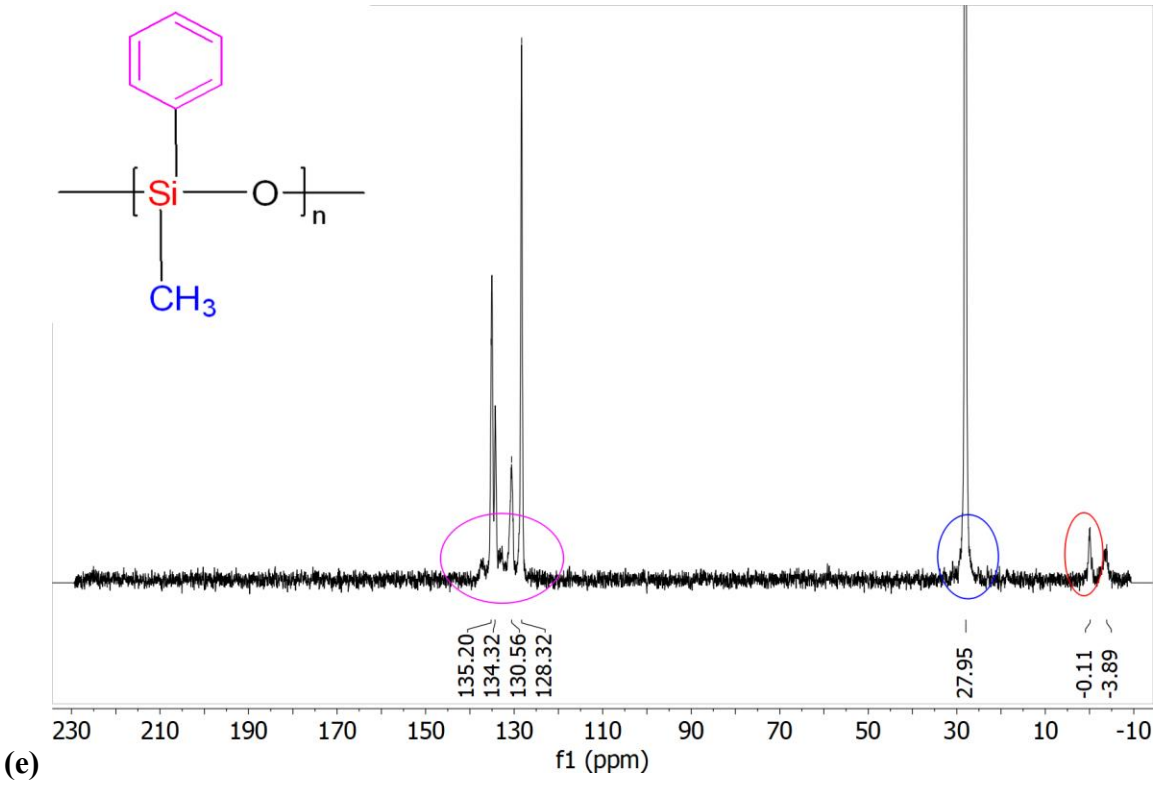

Figure 7. (a) ^{1}H NMR spectra of MK in cyclohexane, **(b)** ^{13}C NMR spectra of MK in cyclohexane, **(c)** ^{29}Si NMR spectra of MK in cyclohexane, **(d)** ^{1}H NMR spectra of H44 in cyclohexane, **(e)** ^{13}C NMR spectra of H44 in cyclohexane. Spectra are enlarged and specific shifts are color coded to correspond to the same color peaks in the spectra.

Figure 7 confirms the different functional groups in the MK and H44 polymers. Figure 7a and b shows various methyl groups in different environments, with no phenyl groups. The peaks around -55 and -60 ppm in Figure 7b confirm the presence of ethoxy groups, as first suggested in the FTIR and Raman analysis. The largest intensity peak in the MK proton and ^{13}C NMR spectra, at 0.1 and 26.77 ppm respectively, is from methyl groups. However, although there are methyl group contributions from both the methyl functional group and the ethoxy group, the peak for the carbon bonded to the oxygen in the ethoxy group, at 1.13 ppm, is much lower than the methyl signal from the methyl group directly attached to the Si, at 0.38 ppm. This high intensity peak indicates a possible higher presence of methyl groups than ethoxy functional groups. Thus, in

crosslinking, bonds are likely formed between the different methyl groups than between the ethoxy functional groups.

Based on Figure 7d and e, peaks in the spectra from H44 correspond with the presence of both methyl and phenyl groups. Specifically, figure 7e has four distinct signals in the aromatic regions, corresponding to the presence of phenyl groups in the H44 polymer. Similar to MK, there is a large signal from the methyl groups, but it is of similar intensity to the contribution from the phenyl groups. Thus, crosslinking during freeze casting may connect both types of functional groups between polymer units, in comparison to how MK likely has bonds between the methyl groups. Given the large size of phenyl groups compared to methyl groups, and the higher energy associated with phenyl groups, additional energy may be required for crosslinking of H44. Another hypothesis could be that crosslinking may occur between methyl groups on the different polymer molecules and thus, in crosslinking H44, given the lower concentration of methyl groups, additional crosslinker may be required for the specific crosslinking mechanism that would connect methyl groups to each other rather than methyl groups to phenyl groups, or phenyl groups to phenyl groups.

Differential scanning calorimetry (DSC)

DSC provides information about the melting and recrystallization behavior of polymers. Specifically, we gain information about the glass transition temperature, or the temperature at which polymers lose their rigidity and start exhibiting viscous behavior, and the melting temperature of the materials. The different endothermic peaks also indicate whether more energy is required during freeze casting; a first order phase transformation at a higher temperature may indicate more energy is required to break bonds in the polymers compared to a material with a lower temperature first order phase transformation.

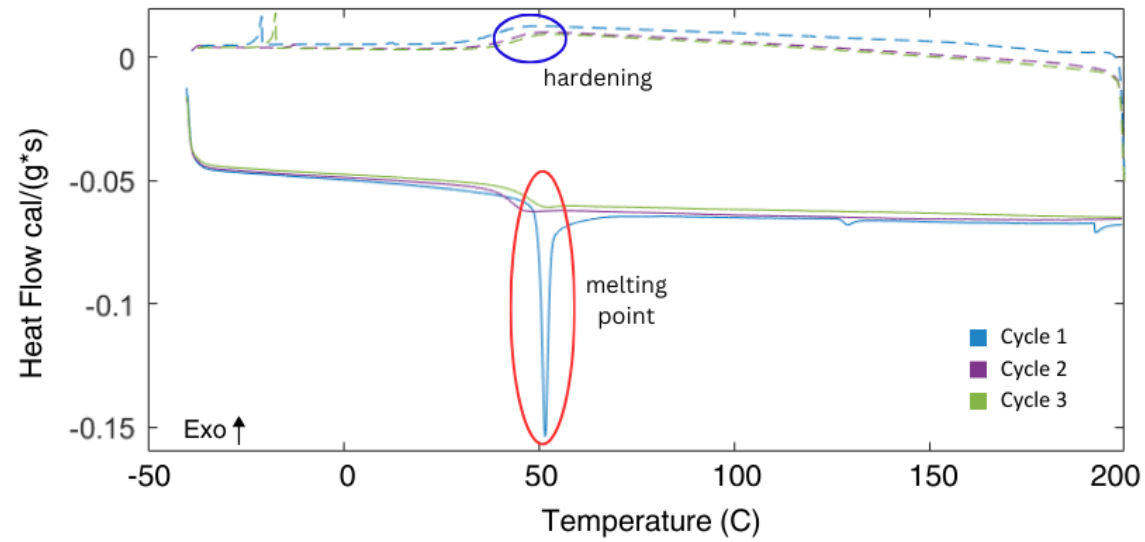

(a)

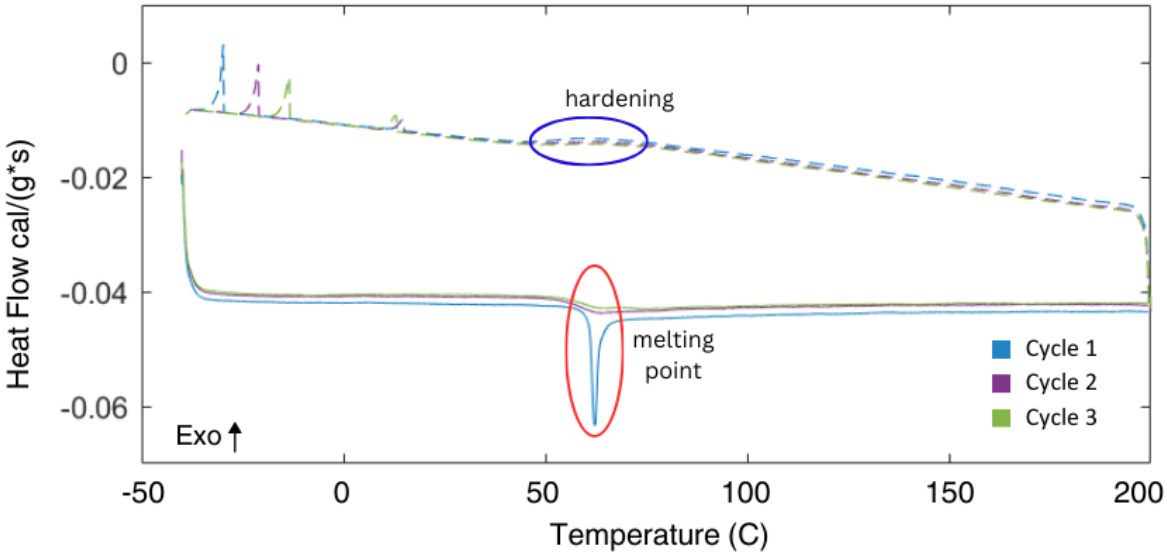

(b)

Figure 8. DSC curves for **(a)** Wacker MK powder and **(b)** Wacker H44 powder, cycled three times between -40°C to 200°C. Cycle for increasing temperature is indicated by a solid line, while the cycle for decreasing temperature are dashed lines.

Sharp endothermic peaks upon heating, in Figure 8, indicate the first order phase transformations occurring in each material. Technical data sheets by Wacker stated these temperatures were a melting point and "softening point" for MK and H44, respectively[22,23]. To verify these temperatures, 2 grams of each preceramic polymer powder were placed in a water

bath at 60℃. Both polymers melted, with the H44 melting earlier. A higher melting point was expected for H44 given the phenyl functionalization, which would require more energy to melt to break intermolecular forces and bonds, compared to the primarily methyl functionalized MK. However, the lower melting point for H44 could indicate that MK has a higher polymerization or monomer count, and thus MK would require more energy than H44 to melt.

Characterization of polymers in solution

Before the polymers were freeze cast and pyrolyzed to create the final silicon oxycarbide structures, they were dissolved in a solvent to create the freeze casting solution. Both MK and H44 were dissolved in cyclohexane before freeze drying.

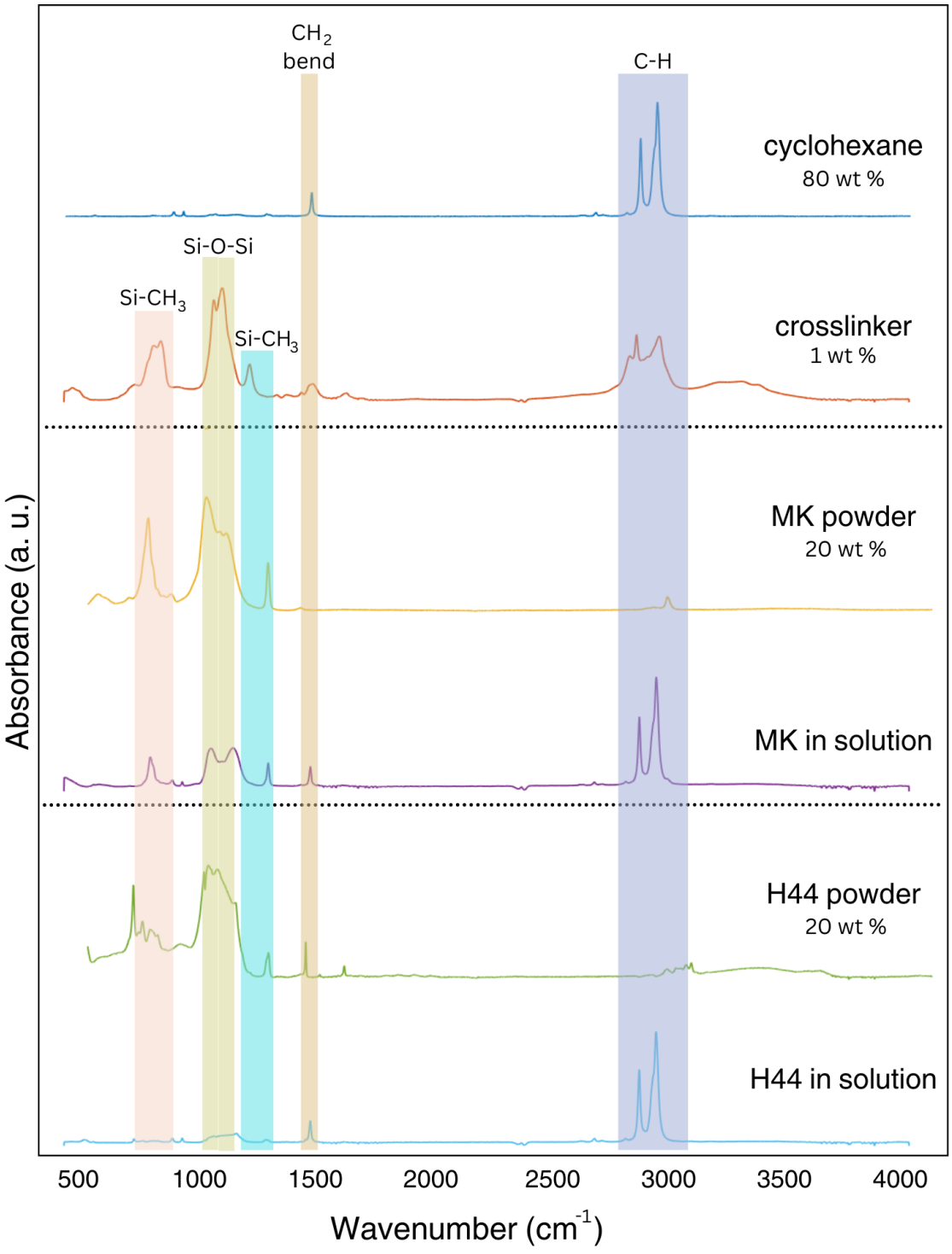

Figure 9. FTIR spectra of MK and H44 in solution, with spectra of cyclohexane (solvent) and crosslinker and weight contributions indicated. Highlighted bands indicate common functional groups and structural bonds across all spectra, labeled at the top of each bar.

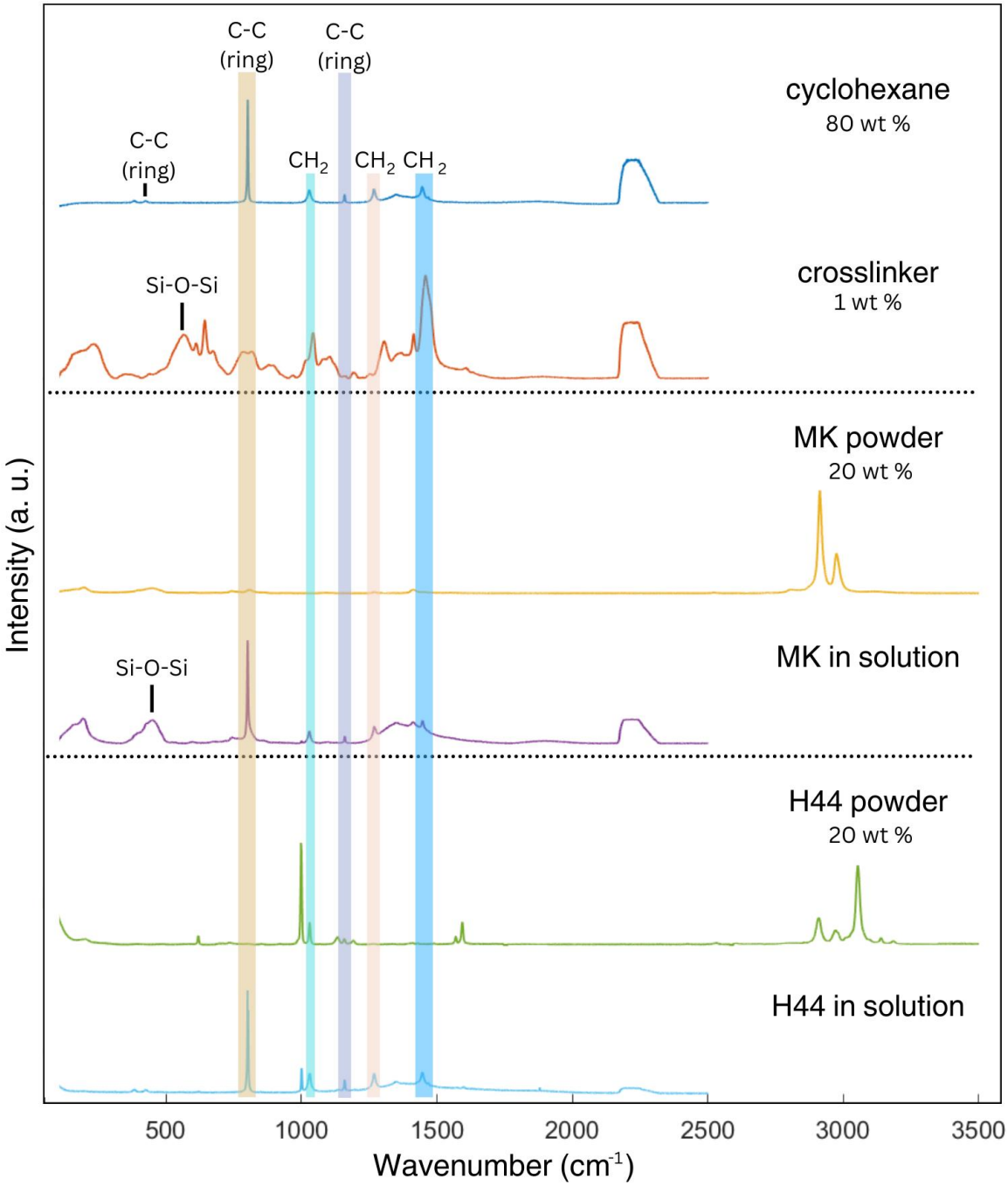

Figure 10. Raman spectra of MK and H44 in solution, with spectra of crosslinker and cyclohexane shown and weight contributions indicated. Highlighted bands indicate common functional groups and structural bonds across multiple spectra, labeled at the top of each bar.

Figures 10 and 11 show the FTIR-ATR and Raman spectra, respectively, of each preceramic polymer as powders and in solution, along with spectra for the solvent (cyclohexane) and the crosslinker GF91 (Wacker Chemie). The solution spectra for each powder shows contributions from the three elements in the system once poured into the mold: preceramic polymer powder, crosslinker, and cyclohexane. Given that cyclohexane is 80 wt% of the solution, the cyclohexane spectra dominates the spectra of the final solutions in both Figure 10 and 11. However, while the spectra for MK in solution still has visible peaks of the MK powder, the spectra for H44 in solution has much lower absorbance and intensity peaks for the H44 powder despite being of the same weight percent as MK. This lower peak absorbance and intensity indicates that H44 is not as concentrated in the freezing solution compared to MK. The low concentration in the final solution could be due to poor dissolution of the polymer, and thus there is less polymer to crosslink and form the porous structure despite initially having the same weight concentration of preceramic polymer. Another hypothesis, informed by the possible low polymerization of H44 as concluded by the DSC analysis, would be that additional facilitation of crosslinking would need to occur to form the H44 polymer network, while the MK already had larger polymer units that did not need to connect to each other via crosslinking as they are already large molecules. In other words, H44 might require a higher crosslinker/H44 ratio as the H44 polymer has a lower polymer chain length and therefore must create more crosslinked bonds for a similar crosslinked structure to MK.

Characterization of preceramic polymer solids

After freeze drying, the preceramic polymers are known as green bodies, or pre-sintered structures that transform into ceramic upon pyrolysis. SEM imaging of MK dissolved in cyclohexane and freeze-dried confirmed the formation of pores, as shown in Figure 12. Based on

the various views in Figure 12, Wacker MK in cyclohexane created a dendritic pore morphology. Although not pyrolyzed, the green bodies still had pores. The Wacker MK freeze-dried sample was noticeably sturdier than the Wacker H44 sample, and thus we were unable to take SEM images of the H44 green bodies. Considering the lower concentration of H44 as seen in the FTIR and Raman spectra of Figure 13, the fragility of the H44 green bodies is hypothesized to be attributed to a failure to fully dissolve enough polymer to have a more robust green body.

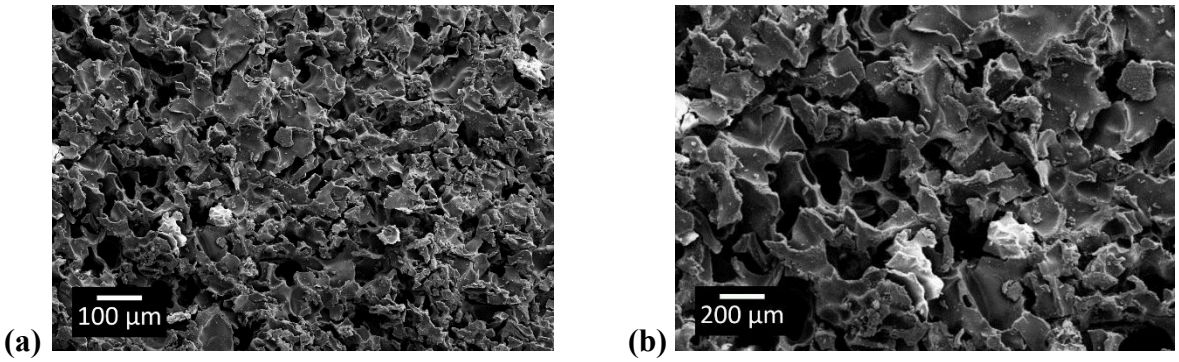

Figure 11. SEM images of freeze-dried structures formed from MK dissolved in cyclohexane, cut along the transverse axis

Upon pyrolysis, as shown in Figure 13, the polymer transformed into a porous silicon oxycarbide ceramic, for both MK and H44.

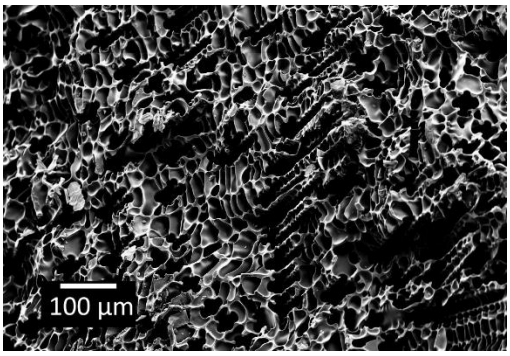

(a)

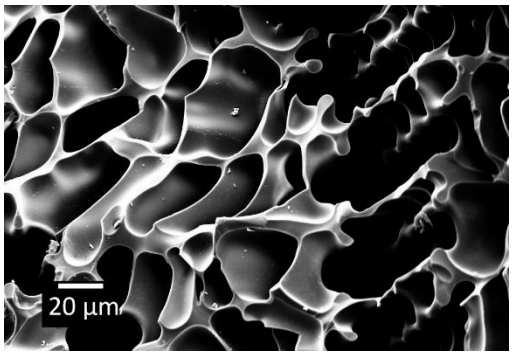

(b)

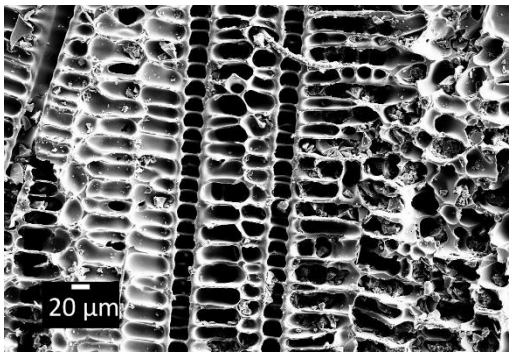

(c)

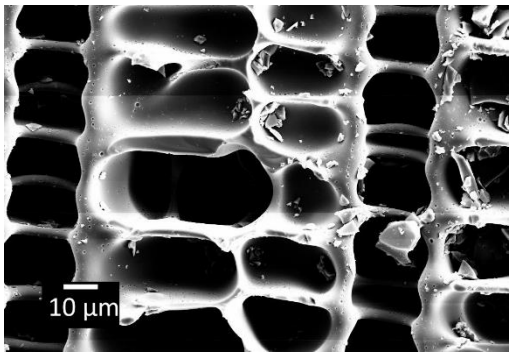

(d)

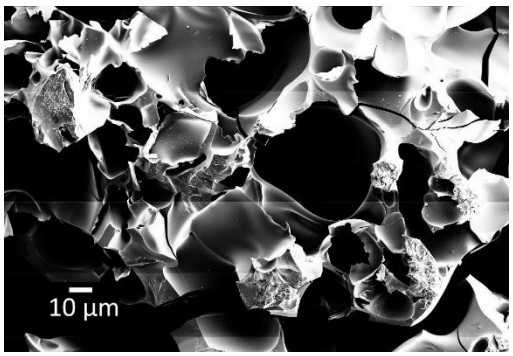

(e)

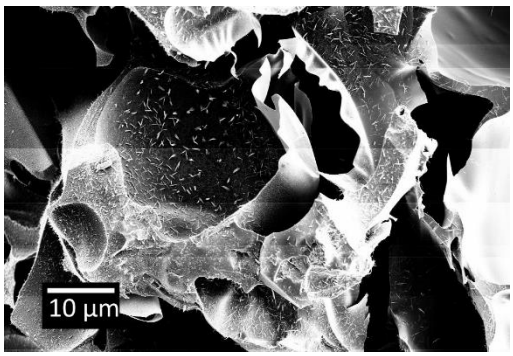

(f)

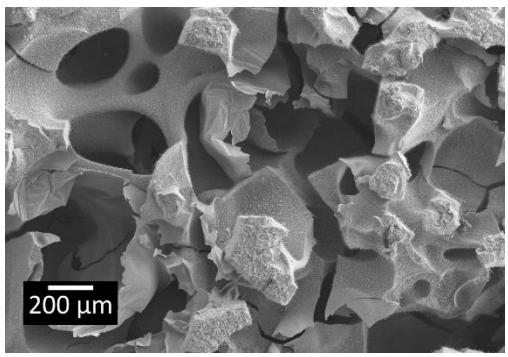

(g)

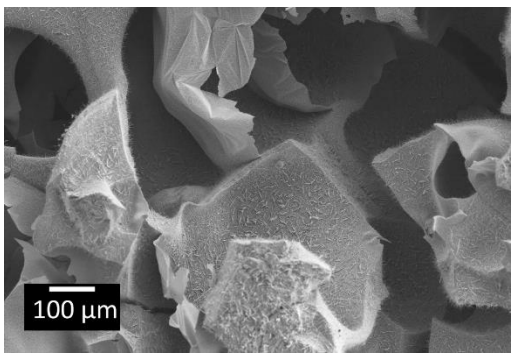

(h)

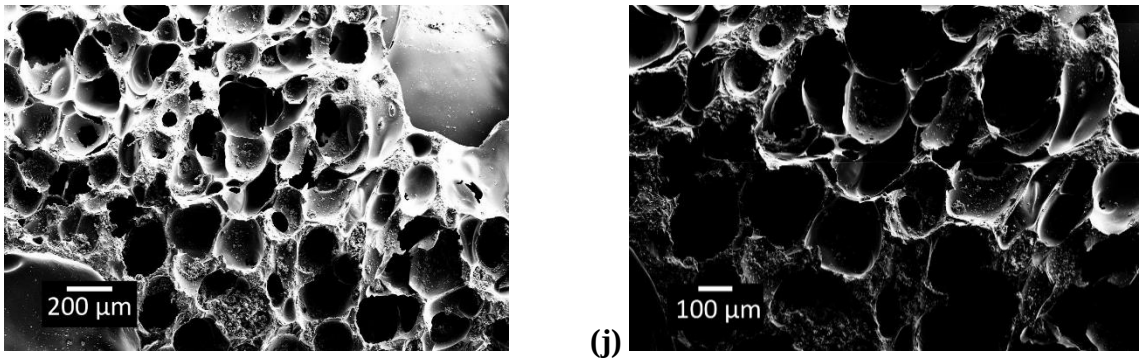

Figure 12. SEM images of (a-d) MK dissolved in cyclohexane with 1 wt% crosslinker, resulting in dendritic pores, (e-f) H44 dissolved in cyclohexane with 1 wt% crosslinker, resulting in dendritic pores, and (g-j) H44 dissolved in cyclooctane, resulting in isotropic pores. Images (a-b, e, g-i) are taken along the transverse axis. Images (c-d, f, j) are all taken on the longitudianal axis of the pyrolyzed structures. H44 images (g-h) used 1 wt% crosslinker during the solution phase, and (i-j) used 2 wt% crosslinker during the solution phase.

The SEM images of Figure 13 indicate the physical transformation of the green bodies into porous ceramic structures. MK was successfully freeze cast in cyclohexane[12] to create the dendritic framework shown in Figure 13a-d, and the final structure is crosslinked with no fractures. The pyrolyzed structures made from H44 as shown in Figure 13 e-i were porous structures, both isotropic pores with cyclooctane and dendritic pores with cyclohexane, but as evidenced by Figure 13g and h, the porous structures are more fragile with numerous breaks along the wall. Figure 13i and j have a more cohesive pore structure, with fewer fractures along the walls compared to Figure 13 g and h. The stronger structure from adding more crosslinker supports the hypothesis that additional crosslinker helped connect the lower concentration of H44 in solution given its poor dissolution, or crosslink the lower polymerized H44 more than with the initial 1 wt% crosslinker.

After freeze drying, FTIR and Raman analysis, as shown in Figure 10 and Figure 11, indicate that the freeze-dried sample is only composed of the polymer, with no trace of the solvent or

crosslinker visible in the spectra. FTIR-ATR and Raman spectroscopy confirm the transformation of the MK and H44 powders from polysiloxanes into silicon oxycarbide.

(a)

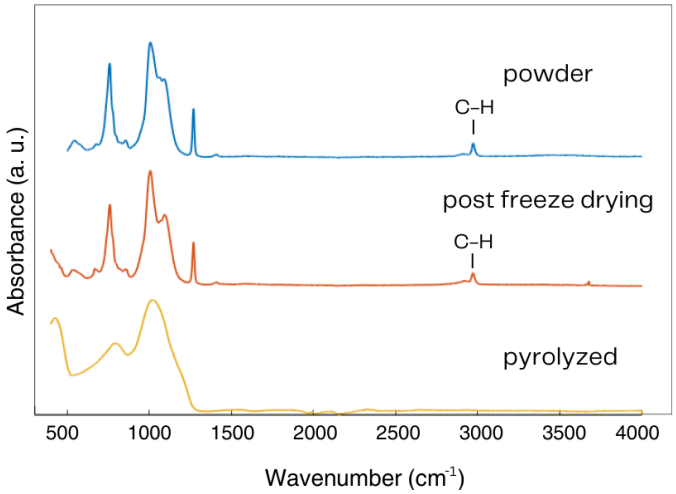

(b)

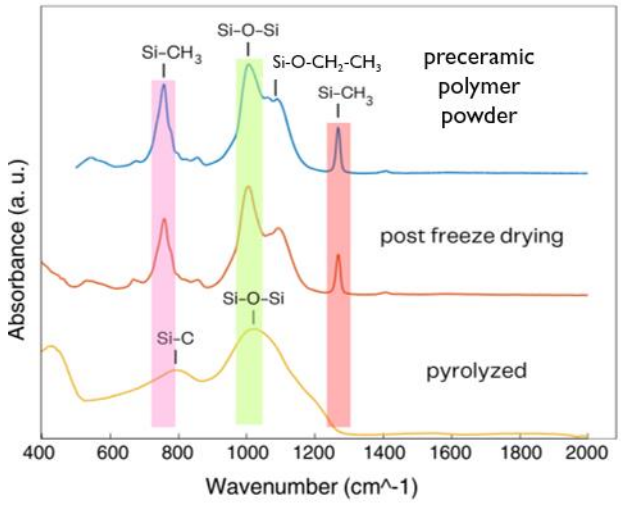

(c)

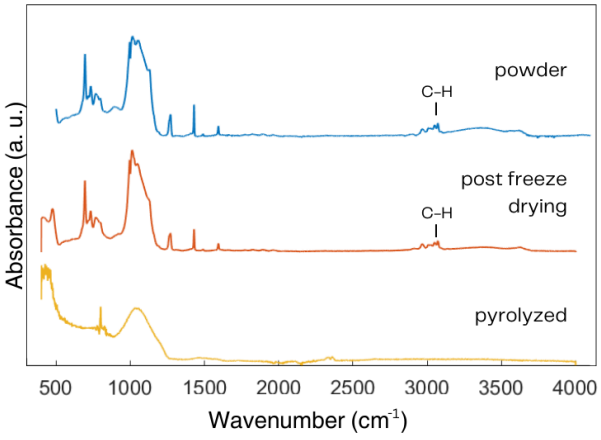

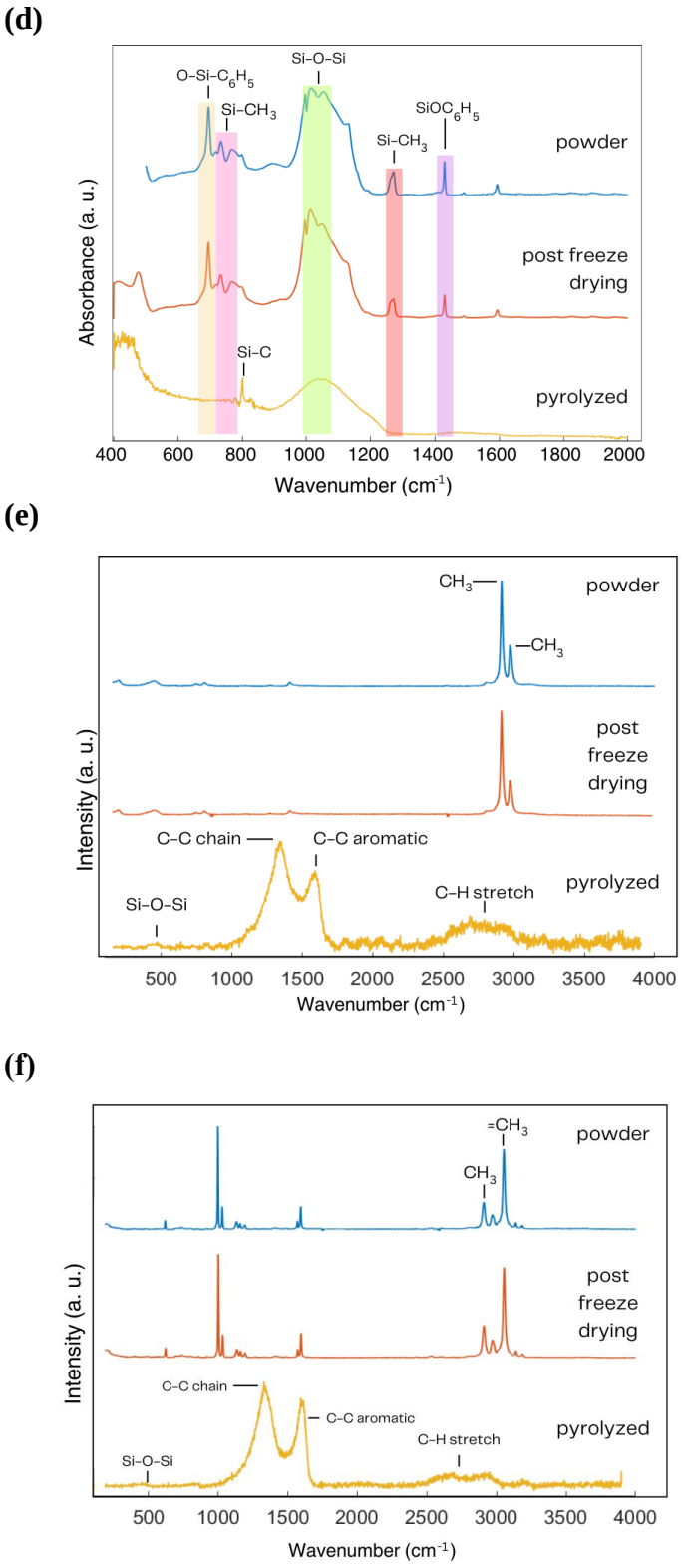

Figure 13. (a-d) FTIR-ATR spectra of **(a-b)** MK and **(c-d)** H44 from powder to pyrolysis, **(e-f)** Raman spectra of **(e)** MK and **(f)** H44 from powder to post pyrolysis.

Figure 14a-d confirm pyrolysis of both preceramic polymers, with no CH_3 peaks in the FTIR spectra for the pyrolyzed sample that were in the powder and post freeze dried spectra. Evident from Figure 14e and f, MK and H44 resulted in compositionally similar silicon oxycarbide final ceramic structures. Although the pore morphologies differed, as seen in Figure 13, the composition analysis suggests that the lack of pore development using H44 was not due to compositional or molecular structural elements of the polymer as it pyrolyzed, but rather due to a low polymer to crosslinker ratio. Adding 2 wt% crosslinker instead of 1 wt% crosslinker improved the pore structure, as shown in Figure 13. This improvement suggests that altering the polymer to crosslinker ratio could facilitate more high energy reactions and improve the pore morphology of freeze-cast siliconoxycarbide ceramics made with H44.

Conclusion

FTIR-ATR, Raman spectroscopy, NMR, and DSC were used to determine preceramic polymer structural changes throughout the freeze-casting process to create porous silicon oxycarbides from polysiloxanes Wacker MK and H44. From these analytical methods, Wacker MK was determined to be a polymethylethoxysiloxane while H44 was determined to be polymethylphenylsiloxane. Although solvents and crosslinkers are used during the freeze-casting process, FTIR-ATR and Raman spectroscopy confirmed that the ceramic green body before pyrolysis is primarily composed of the preceramic polymer as there were no peaks from the solvent or crosslinker present in spectra taken of the green bodies. This confirms a full phase separation of the solvent and polymer during the freezing stage, and full sublimation of the solvent during

freeze drying. Additionally, the lack of solvent and crosslinker in the green body spectra confirms that no solvent or crosslinker is pyrolyzed, so the final product is only a result of the polymer powders.

As seen from SEM imaging, pore morphology develops in the ceramic green bodies as a result of freeze casting and is preserved through pyrolysis. While porous structures made with MK were solid and connected structures, those made with H44 with the same crosslinker/polymer ratio resulted in fractures along the pore walls. However, adding additional crosslinker helped facilitate crosslinking with the high energy phenyl groups and prevented pore wall fracture, as initially occurred. Raman spectroscopy and FTIR-ATR confirmed the successful conversion of both polysiloxanes into siliconoxycarbides. The successful conversion indicates that improving the pore characteristics of freeze-cast structures with H44 can be developed through optimization of the crosslinker/polymer ratio. Both MK and H44 successfully freeze-cast porous silicon oxycarbide structures. Future research may explore optimizing the crosslinker/H44 ratio further to better improve the pore characteristics, concepts which can then be applied to other preceramic polysiloxanes or other polymers.

Works Cited

1. Colombo, P. Conventional and novel processing methods for cellular ceramics. *Philos. Trans. R. Soc. Math. Phys. Eng. Sci.* **364**, 109–124 (2005).
2. Lv, Y. *et al.* Silver nanoparticle-decorated porous ceramic composite for water treatment. *J. Membr. Sci.* **331**, 50–56 (2009).
3. Sebastian, M. T., Wang, H. & Jantunen, H. Low temperature co-fired ceramics with ultra-low sintering temperature: A review. *Curr. Opin. Solid State Mater. Sci.* **20**, 151–170 (2016).
4. Wu, C.-W. V. Freeze Casting - from Battery Separators to Ceramic Scaffolds. (California Institute of Technology, 2023). doi:10.7907/ghvz-q712.
5. Elsayed, H., Zocca, A., Franchin, G., Bernardo, E. & Colombo, P. Hardystonite bioceramics from preceramic polymers. *J. Eur. Ceram. Soc.* **36**, 829–835 (2016).
6. Bellucci, D., Sola, A. & Cannillo, V. A Revised Replication Method for Bioceramic Scaffolds. *Bioceram. Dev. Appl.* **1**, 1–8 (2011).
7. Galante, R., Figueiredo-Pina, C. G. & Serro, A. P. Additive manufacturing of ceramics for dental applications: A review. *Dent. Mater.* **35**, 825–846 (2019).
8. Chari, C. S. Degradation of Ceramic Surfaces and its Mitigation: From Electric Propulsion to Cultural Heritage. (California Institute of Technology, 2023). doi:10.7907/22st-q436.
9. Colombo, P., Mera, G., Riedel, R. & Sorarù, G. D. Polymer-Derived Ceramics: 40 Years of Research and Innovation in Advanced Ceramics: Polymer-Derived Ceramics. *J. Am. Ceram. Soc.* no-no (2010) doi:10.1111/j.1551-2916.2010.03876.x.
10. Mott, M. & Evans, J. R. G. Solid Freeforming of Silicon Carbide by Inkjet Printing Using a Polymeric Precursor. *J. Am. Ceram. Soc.* **84**, 307–13 (2001).

11. Nangrejo, M. R., Bao, X. & Edirisinghe, M. J. Preparation of silicon carbide–silicon nitride composite foams from pre-ceramic polymers. *J. Eur. Ceram. Soc.* **20**, 1777–1785 (2000).
12. Naviroj, M., Miller, S. M., Colombo, P. & Faber, K. T. Directionally aligned macroporous SiOC via freeze casting of preceramic polymers. *J. Eur. Ceram. Soc.* **35**, 2225–2232 (2015).
13. Riedel, R., Mera, G., Hauser, R. & Klonczynski, A. Silicon-Based Polymer-Derived Ceramics: Synthesis Properties and Applications-A Review. *J. Ceram. Soc. Jpn.* **114**, 425–444 (2006).
14. Miranda, I. *et al.* Properties and Applications of PDMS for Biomedical Engineering: A Review. *J. Funct. Biomater.* **13**, 2 (2021).
15. Manoj Kumar, B. V. & Kim, Y.-W. Processing of polysiloxane-derived porous ceramics: a review. *Sci. Technol. Adv. Mater.* **11**, 044303 (2010).
16. Sorar, G. D., Campostrini, R., Maurina, S. & Babonneau, F. Gel Precursor to Silicon Oxycarbide Glasses with Ultrahigh Ceramic Yield. *J. Am. Ceram. Soc.* **80**, 999–1004 (1997).
17. Scheffler, M. & Colombo, P. *Cellular Ceramics: Structure, Manufacturing, Properties and Applications*. (John Wiley & Sons, 2006).
18. Kim, Y. *et al.* Nanoporous SiC Membrane Derived from Preceramic Polymer. *Solid State Phenom.* **124–126**, 1733–1736 (2007).
19. Arai, N. Freeze Casting of Ceramics: Pore Design from Solidification Principles. (California Institute of Technology, 2021). doi:10.7907/3rmr-cz93.
20. Kuo, C. T. Customized Porosity in Ceramic Composites via Freeze Casting. (California Institute of Technology., 2021). doi:10.7907/88p1-5v79.

21. Gokuli, M. A Combined High Temperature Tape-Casting and 2D Freeze-Casting Method for Polymer Membranes with Vertically Oriented Pores. (California Institute of Technology, 2021). doi:10.7907/ywpf-cx09.
22. SILRES® MK POWDER | Silicone Resins | Wacker Chemie AG. *WACKER Website* https://www.wacker.com/h/en-us/silicone-resins/silicone-resins/silres-mk-powder/p/000008049.
23. SILRES® H44 | Silicone Resins | Wacker Chemie AG. *WACKER Website* https://www.wacker.com/h/en-us/silicone-resins/silicone-resins/silres-h44/p/000002761.
24. Gulmine, J. V., Janissek, P. R., Heise, H. M. & Akcelrud, L. Polyethylene characterization by FTIR. *Polym. Test.* **21**, 557–563 (2002).
25. Patacsil, C. Hydrophobicity and FTIR absorbance spectroscopy of Polydimethylsiloxane (PDMS) films treated with aqueous gold nanoparticles (AuNP) solution. *Mater. Today Proc.* (2023) doi:10.1016/j.matpr.2023.05.449.
26. Badr, Y., Ali, Z. I. & Khafagy, R. M. On the mechanism of low temperature glass transition in low density polyethylene films. *Radiat. Phys. Chem.* **58**, 87–100 (2000).
27. Bistričić, L., Borjanović, V., Mikac, L. & Dananić, V. Vibrational spectroscopic study of poly(dimethylsiloxane)-ZnO nanocomposites. *Vib. Spectrosc.* **68**, 1–10 (2013).
28. Botelho do Rego, A. M., Pellegrino, O. & Vilar, M. R. Vibrational and Electronic Excitations in Poly(methylphenylsilane) and Poly(diphenylsiloxane) Films: Surface Aspects. *Macromolecules* **34**, 4987–4992 (2001).
29. Verevkin, S. P. Strain effects in phenyl substituted methanes. Geminal interactions between phenyl and alkoxycarbonyl substituent. *Thermochim. Acta* **332**, 27–32 (1999).